Electronic Supplementary Information (ESI) for

Hierarchical 3D TiO$_2$@Fe$_2$O$_3$ nanoframework arrays as high-performance anode materials

Lin Gao, Hao Hu, Guojian Li, Qiancheng Zhu and Ying Yu*

Experimental details

Preparation of TiO$_2$ arrays:

After cleaning by sonication in alcohol and acetone for three times, Ti substrate (50×30×0.2 mm^3) was placed against the wall of Teflon-lined stainless-steel autoclave (100 mL) containing 40 mL 1M NaOH solution and different concentration of NaCl (0, 1M, 2M and 3M) for the preparation of TiO$_2$ samples with different morphologies). Then it was held in the oven at 200 °C for 12 h, followed by being immersed in a dilute HCl solution (0.5 M) for 30 mins to replace Na$^+$ with H$^+$. The film was subsequently calcined at 500 °C for 1 h to synthesize crystallized TiO$_2$ nanosheet arrays.

Preparation of Fe$_2$O$_3$ nanorod arrays and TiO$_2$@Fe$_2$O$_3$ arrays:

The calcined TiO$_2$ arrays prepared by hydrothermal reaction with 40 mL NaOH solution (1M) were placed in three Teflon-lined autoclaves with 9.3 mM FeCl$_3$·6H$_2$O, 17.6 mM Na$_2$SO$_4$; 18.6 mM FeCl$_3$·6H$_2$O, 35.2 mM Na$_2$SO$_4$; 25 mMFeCl$_3$·6H$_2$O, 24.6 mM Na$_2$SO$_4$. They had been kept in an oven at 120 °C for 8 h. After calcination at 500 °C for 1 h, the obtained TiO$_2$-Fe$_2$O$_3$ arrays were directly used to assemble the electrode. Fe$_2$O$_3$ nanorod arrays were prepared by placing Ti substrate in Teflon-lined autoclave only containg18.6 mM FeCl$_3$·6H$_2$O and 35.2 mM Na$_2$SO$_4$ for hydrothermal reaction at 120 °C for 8 h.

Characterization:

The crystalline phase of the prepared samples were characterized by X-ray diffraction (XRD, Bruker D8-advance, Germany, Cu KR radiation; λ=1.5418 Å) from 10°~ 80°.

The mean pore size distribution and specific surface area were tested by means of Barret-Joyner-Halenda (BJH) using a BELSORP-mini (BEL) instrument. Field emission scanning electron microscopy (FESEM JEOL JSM-6700F) and transmission electron microsopy (TEM, Tecnai G2 20 U-Twin) were employed to determine the morphology of samples.

The process for assembling half cells is as follow. The prepared products were punched to wafers with diameter of 14 mm and assembled to 2016 half coin cells with Li metal as the counter electrode and polypropylene as the separator. The electrolyte LiPF6 (1 M) was dissolved in a mixture of ethylene carbonate (EC), ethylmethyl carbonate (EMC) and dimethyl carbonate (DMC) with a volume ratio of 1:1:1. All of the coin cells were assembled in a air-filled glove box (Mbraun) and detected using a BTS-55 Neware battery testing system (Shenzhen, China) at room temperature with the voltage window of 0.05~3 V (vs. Li/Li$^+$) at various current densities. The alternation current (AC) impedance was measured from the frequency of 100 kHz to 0.1 Hz on a CS350 electrochemical machine system (Wuhan, China) with voltage amplitude of 5 mV.

Supplementary Figures
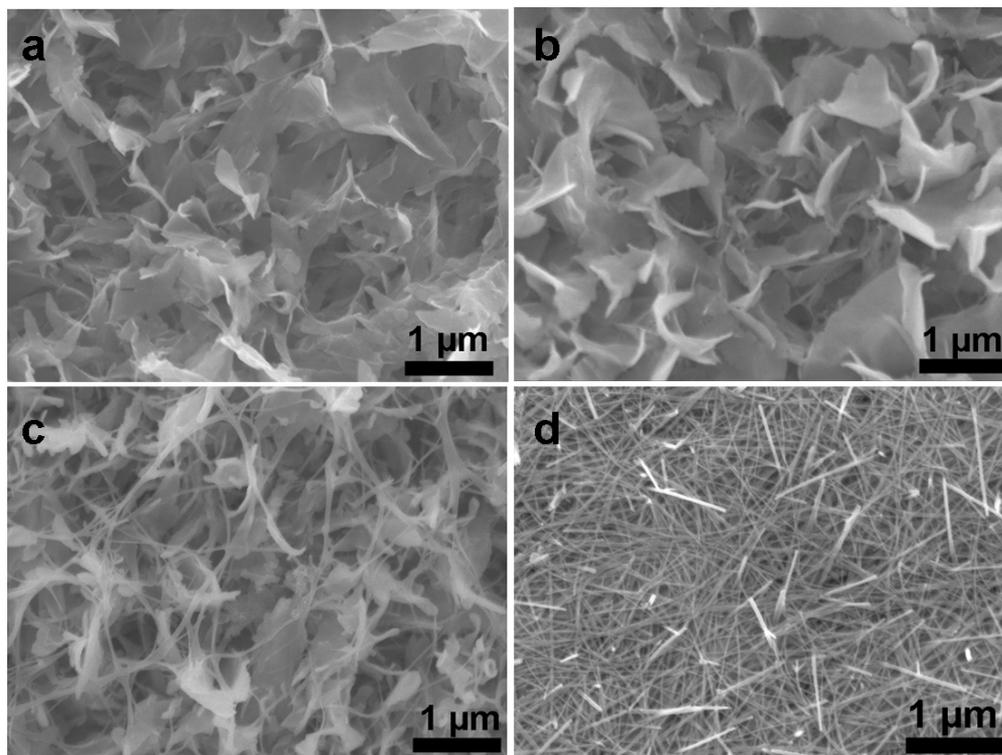
Fig. S1. SEM images of TiO_2 arrays prepared with different concentration of NaCl solution: (a) 0 M, (b) 1 M, (c) 2 M and (d) 3 M.
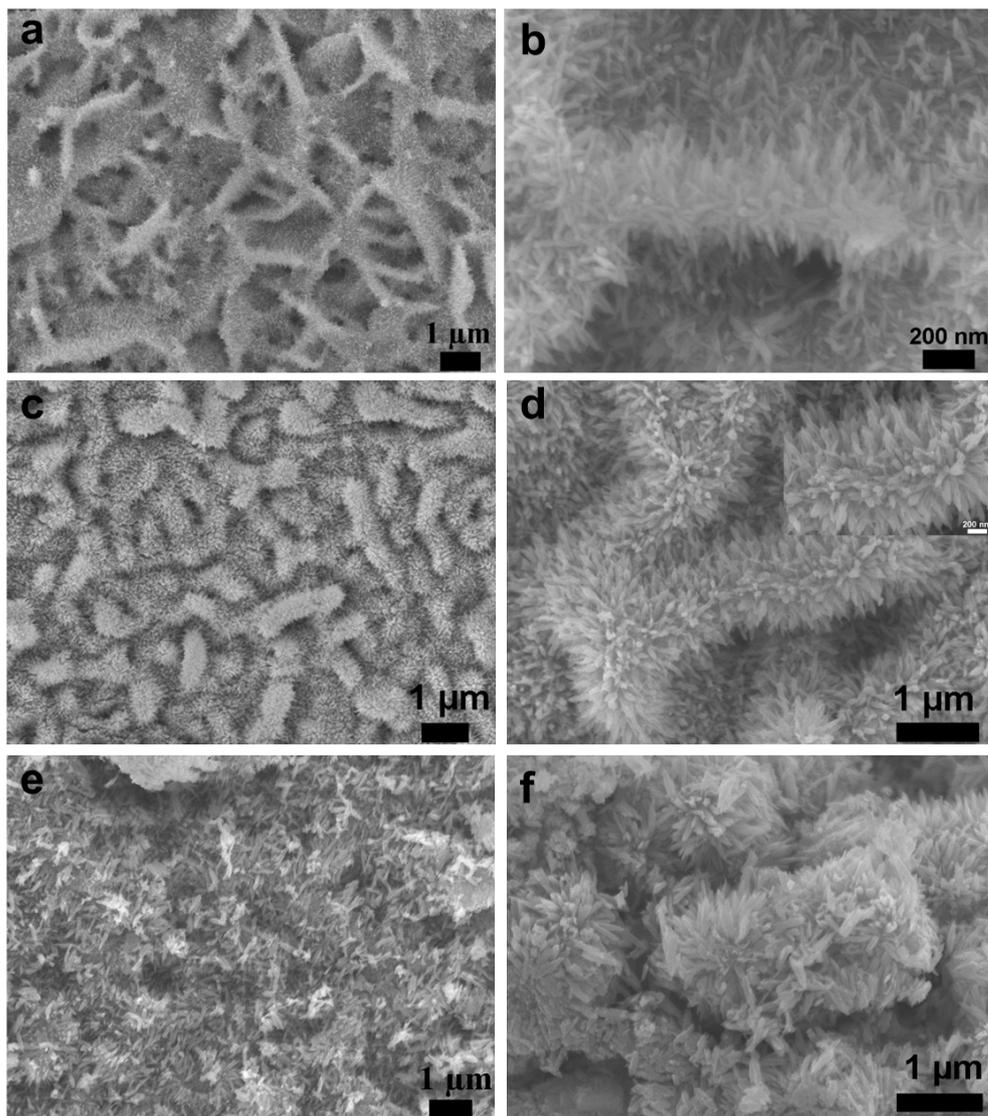
Fig. S2. SEM images of $TiO_2@Fe_2O_3$ nanoframework arrays prepared with different contents of $FeCl_3 \cdot 6H_2O$ and Na_2SO_4: (a, b) 9.3 mM $FeCl_3 \cdot 6H_2O$ and 17.6 mM Na_2SO_4, (c, d) 18.6 mM $FeCl_3 \cdot 6H_2O$ and 35.2 mM Na_2SO_4 and (e, f) 25 mM $FeCl_3 \cdot 6H_2O$ and 24.6 mM Na_2SO_4.
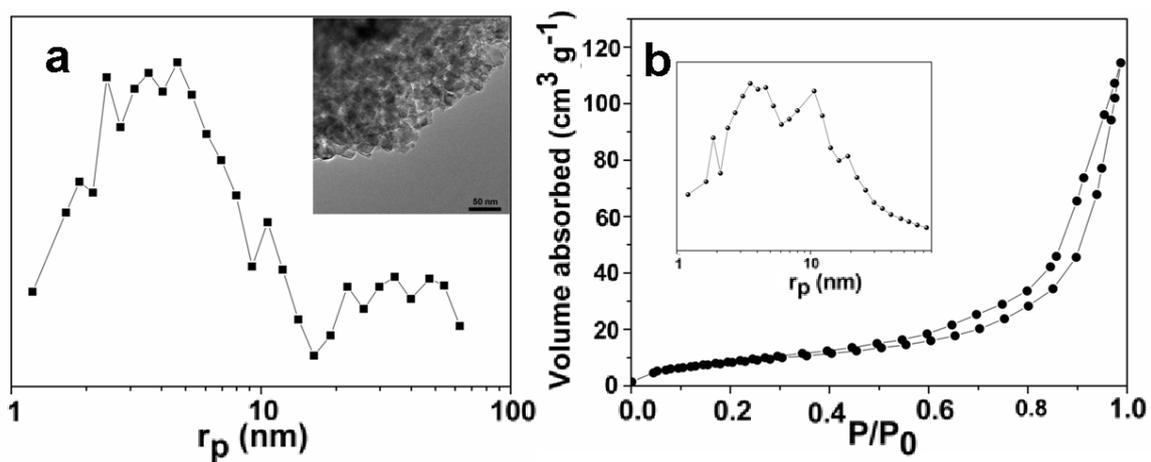
Fig. S3. (a) Pore size distribution of TiO$_2$ nanosheet arrays (The inset is the enlarged TEM image of TiO$_2$ nanosheet arrays) and (b) N$_2$ adsorption-desorption curve of TiO$_2$@Fe$_2$O$_3$ nanoframework arrays (The inset is the pore diameter distribution).
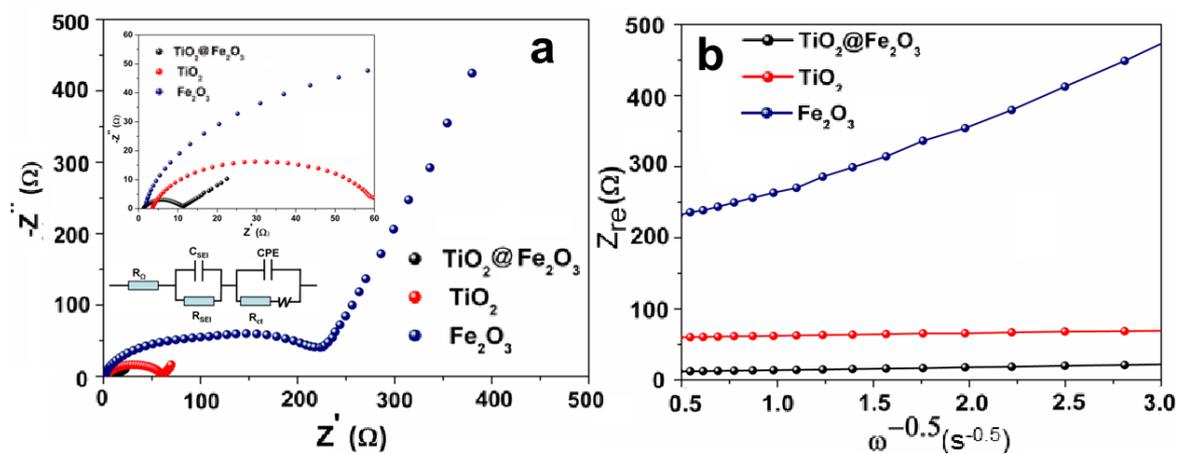
Fig. S4. (a) Nyquist plots before cycling for pristine $TiO_2@Fe_2O_3$, TiO_2 and Fe_2O_3 electrodes (The inset is the magnified nyquist plots and equivalent circuit model) and (b) the relation between low frequency and real resistance for $TiO_2@Fe_2O_3$, TiO_2 and Fe_2O_3 electrodes.
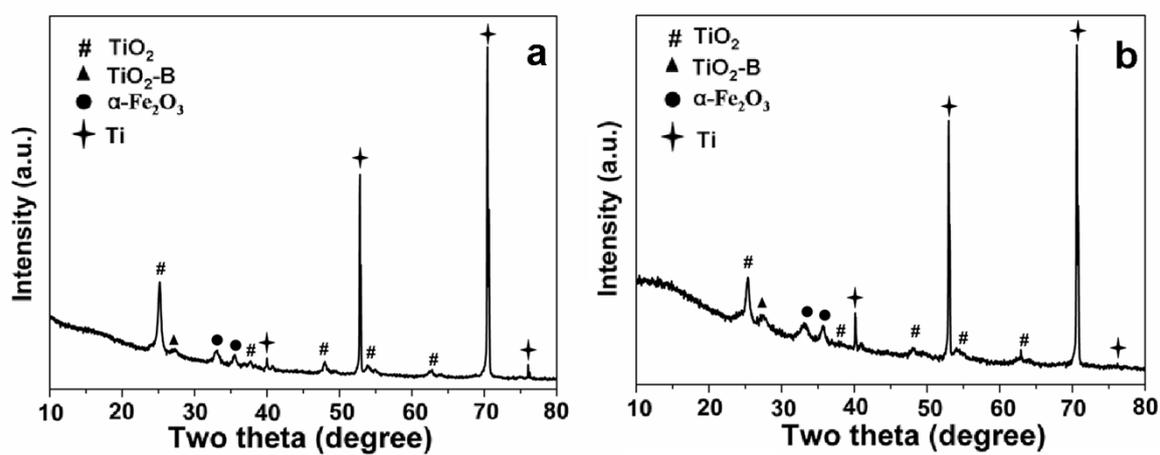
Fig. S5. XRD patterns of the samples prepared with (a) 9.3 mM $FeCl_3 \cdot 6H_2O$ and 17.6 mM Na_2SO_4 and (b) 18.6 mM $FeCl_3 \cdot 6H_2O$ and 35.2 mM Na_2SO_4.
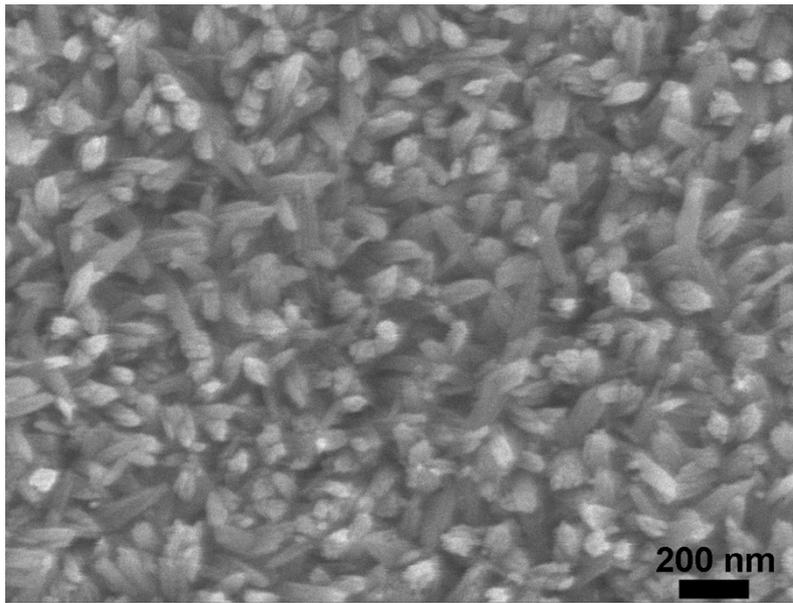
Fig. S6. SEM image for the top view of Fe_2O_3 nanorod arrays on Ti substrate.
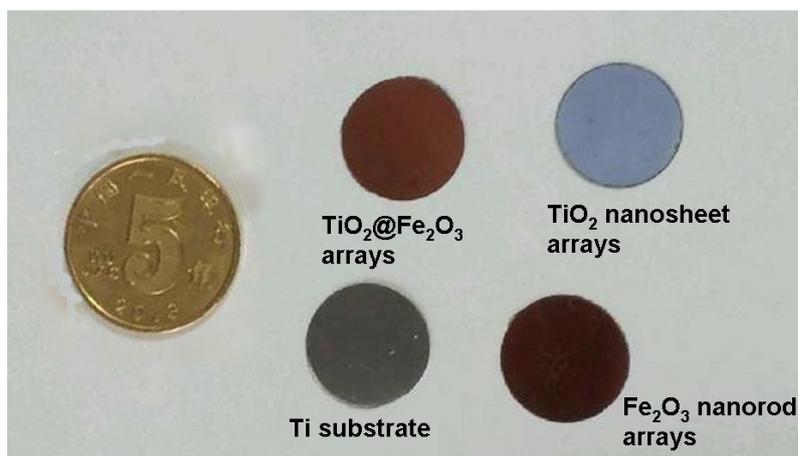
Fig. S7. Optical image of Ti substrate and prepared arrays (Chinese coin used as a scale bar).
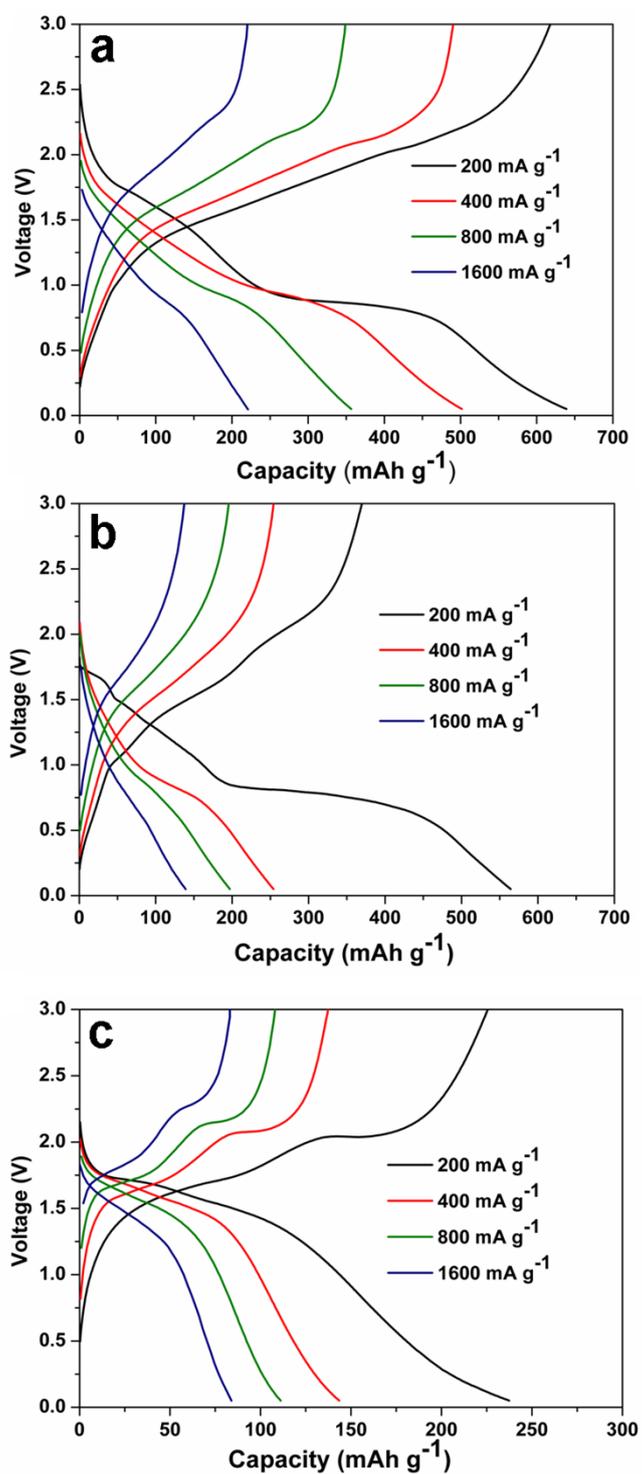
Fig S8. Galvanostatic charge-discharge curves for (a) $TiO_2@Fe_2O_3$, (b) Fe_2O_3 and (c) TiO_2 electrodes at various current densities.
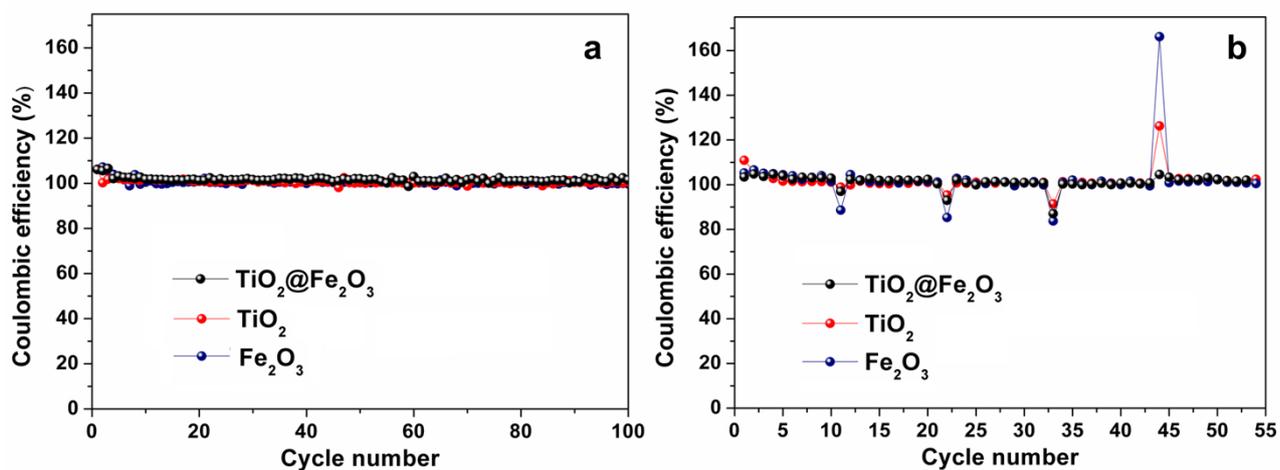
Fig. S9. Coulombic efficiency of three electrodes corresponding to (a) cycling performance and (b) rate performance. The sharp noise in (b) was attributed to the change of the current density during rate performance measurement.